MALACOLOGIA, 2012, 55(1): 43–54

LONGEVITY AND GROWTH RATES OF THE GUMBOOT CHITON, *CRYPTOCHITON STELLERI*, AND THE BLACK LEATHER CHITON, *KATHARINA TUNICATA*

Joshua P. Lord

University of Connecticut Department of Marine Sciences; 1080 Shennecossett Rd., Groton, Connecticut 06340-6048, U.S.A.; joshua.lord@uconn.edu

ABSTRACT

Few studies have documented chiton growth rates, and lifespans for most chiton species remain unknown. This study presents the first size-at-age and longevity estimates for *Cryptochiton stelleri* and *Katharina tunicata*, two of the largest known species of chitons. Age estimates were based on growth ring counts obtained by cross-sectioning and polishing valves. This process alone showed clear growth rings in shell plates of *K. tunicata.* Valves of *C. stelleri* did not show conspicuous growth rings in cross section, so the acetate peel technique was used to highlight growth bands. Linear growth in terms of body length and shell width approached an asymptote in both species and was described with the von Bertalanffy growth function. Both *C. stelleri* and *K. tunicata* displayed indeterminate growth with regard to tissue weight and shell weight, continuing to maintain a steady growth rate throughout their lifespans. The oldest *K. tunicata* specimen was estimated to be 17 years old. The oldest *C. stelleri* was estimated to be 40 years old, making it the longest-lived chiton species known.

Key words: mollusk, age, lifespan, sclerochronology, growth.

INTRODUCTION

Growth rate is one of the most fundamental life history parameters and is critical in developing models of the overall health, structure, and reproductive output of a population. Comprehensive knowledge of population structure is vital to the understanding of population dynamics for any species, especially those that are long-lived, because size and longevity impact the lifetime reproductive output of an individual or population (O'Farrell & Botsford, 2005). Growth rate information is available for many marine organisms, especially those with commercial value, such as fish and bivalves (Gang et al., 2008; Abele et al., 2009). Despite the relative abundance of growth rate data in general, established growth curves for some marine invertebrates are less common. This is particularly true for the chitons, class Polyplacophora.

The gumboot chiton, *Cryptochiton stelleri* (Middendorff, 1846), and the black leather chiton, *Katharina tunicata* (Wood, 1815), are fairly common inhabitants of the intertidal zone throughout their shared range (Japan and Kamchatka to Alaska and down the Pacific Northwest coast to central California) (Himmelman, 1978; Yates, 1989). It is well-known that *C. stelleri* is the largest species of chiton in the world, at up to 36 cm long and up to 2,000 g (Lord, 2011b), and it feeds on a variety of seaweeds, including the algal genera *Cryptopleura, Mazzaella, Ulva, Nereocystis,* and *Odonthalia* (Yates, 1989; DeBusk et al., 2000). Like *C. stelleri*, *K. tunicata* feeds largely on macroalgae, in this case the kelp *Saccharina sessilis* and occasionally erect coralline algae or other leafy seaweed (Dethier & Duggins, 1984). *Katharina tunicata* can reach a length of up to 12 cm, making it the second largest chiton (to *C. stelleri*) in the northeastern Pacific (Himmelman, 1978). The only published study on the age or growth of *K. tunicata* was done by Heath (1905), who estimated that this species could live for three years in central California. The same study estimated *C. stelleri* lifespan at four years, but later studies have suggested that this chiton may live considerably longer.

Multiple studies have focused on the growth rate of *C. stelleri*, but few conclusions have been reached. Studies by MacGinitie & MacGinitie (1968) and Palmer & Frank (1974) attempted to use growth lines on the outside of the valves to determine age of this species, but the researchers ultimately decided that these lines were too obscure to use for aging purposes. Despite the inability to fully interpret the growth lines, a number of studies have suggested that *C. stelleri* is quite long-lived, living up to 20 years or more (MacGinitie & MacGinitie, 1968; Palmer & Frank, 1974; Yates, 1989). However, Palmer & Frank (1974) expressed doubts about the external growth ring method used by MacGinitie & MacGinitie (1968) to arrive at the estimate of 20 years. Lord (2011a) documented the juvenile growth rate of *C. stelleri*, but did not attempt to describe adult growth. As such, little is known about the growth and longevity of *C. stelleri* and even less about the growth patterns of *K. tunicata*. This is partly due to the flexible morphology of chitons (especially *C. stelleri* and *K. tunicata*), which makes measurements of length highly variable.

The present study closely examined the ontogeny and growth rates of *C. stelleri* and used the growth rates of juveniles and young individuals to support age estimates based on growth rings. It was hypothesized that internal shell growth rings could be used to approximate age in *C. stelleri* and *K. tunicata* and would reveal longer lifespans than previously reported, given the large size of these chitons. A wide range of morphological measurements were used to facilitate the first detailed description of growth for the largest chitons in the world, *Cryptochiton stelleri* and *Katharina tunicata.*

MATERIALS AND METHODS

This study was conducted primarily along the central Oregon coast. *Katharina tunicata* specimens (n = 40) that were measured and sacrificed were taken from South Cove, Cape Arago, Oregon, ten km south of Charleston, Oregon (43°18.191'N, 124°23.198'W). *Cryptochiton stelleri* individuals that were sacrificed in order to measure the growth rings in their valves were taken from Lighthouse Island, Sunset Bay, and Cape Arago, all near Charleston, Oregon. Only nine *C. stelleri* were taken from each site in January 2010 in order to minimize collecting impact. The majority of the valves that were used to analyze growth lines were from individuals that washed up dead on the beach, so were not killed for the purpose of this study. In February 2009, 32 dead *C. stelleri* were collected from a beach near Fort Ebey State Park, Washington, and 12 individuals were collected from the south end of Asilomar Beach near Monterey, California in December 2009.

Cryptochiton stelleri that were washed up on the beaches in Washington and California were too deteriorated to obtain any body size information, so all external body measurements were done solely on individuals from the sites in Oregon. All size and age data for *K. tunicata* were from the specimens collected at the south cove of Cape Arago in Charleston, Oregon. The *C. stelleri* shell data were pooled from all sites on the southern Oregon coast (10 km range) and were analyzed separately from the shells of the specimens collected near Fort Ebey, Washington, and Monterey, California. External measurements included body length (*K. tunicata*) and circumference when curled up in a ball (*C. stelleri*). Body length of *K. tunicata* was measured along the longest axis, from the front to the back of the girdle when the specimens were relaxed, with an accuracy of 1 mm.

Circumference was used for *C. stelleri* because of its flexible morphology and was determined by first picking up and holding specimens until they were tightly curled and then measuring the circumference longitudinally to the nearest millimeter. The reliability of this method was verified by making repeated measurements of 15 specimens, which were given time to uncurl between each measurement. Volume (water displacement) and weight in air were also measured for *C. stelleri* and *K. tunicata*. All specimens were kept in a flowing seawater table for a week prior to measurement so that weight and volume measures would not be biased by environmental factors. During this time, seaweeds *Mazzaella splendens* and *Sacharina sessilis* were fed to *C. stelleri* and *K. tunicata*, respectively.

Specimens were relaxed, then killed with a 7.5% magnesium chloride solution the same day external measurements were taken and one week after field collection. Valves were removed, cleaned and dried for two weeks, weighed on a digital scale and then photographed and measured digitally using ImageJ (available at http://rsb.info.nih.gov/ij). The valve measurements, length (at the shortest point) and width (at the widest point), were made on the third, fourth and fifth valves for each *Katharina tunicata* specimen (Fig. 1). Using multiple valves per specimen improved the reliability of the growth ring counts for each individual, and these three valves were the largest and easiest to handle for *K. tunicata*. The same length, width and weight measurements were made on all intact valves from California, Oregon, and Washington *Cryptochiton stelleri*, for a total of over 300 valves measured and weighed from

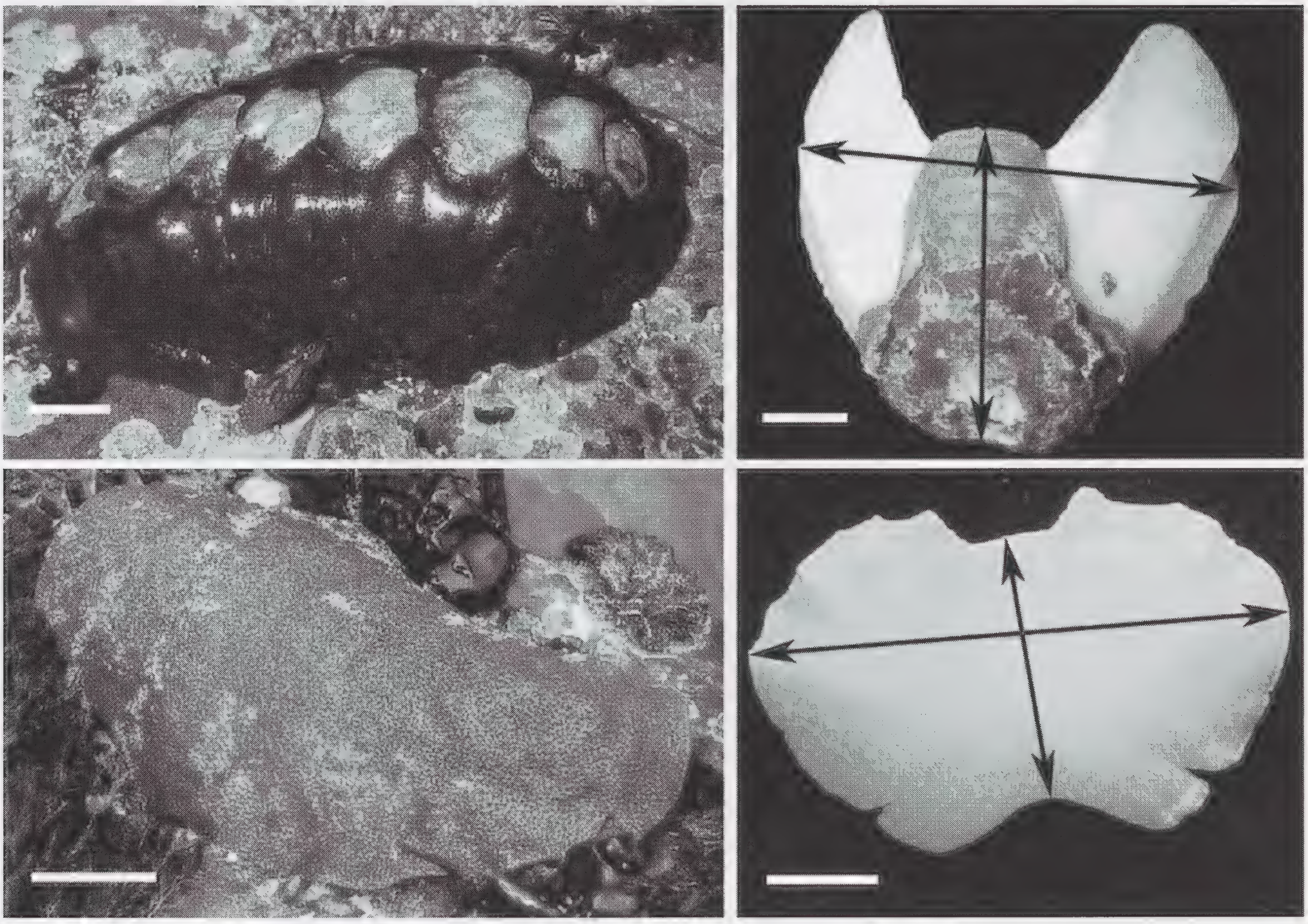

FIG. 1. Dorsal views of *Katharina tunicata* (upper left, scale = 1 cm) and *Cryptochiton stelleri* (lower left, scale = 5 cm) in the intertidal zone in central Oregon. Top-down views *K. tunicata* (upper right, scale = 5 mm) and *C. stelleri* (lower right, scale = 1 cm) valves are pictured after dissection and cleaning. Valves were cross-sectioned along the axes indicated by arrows.

71 individuals. Because many of the Washington and California specimens that had washed up in the intertidal zone had several broken valves (approximately 58% of valves were broken) (excluded from analysis), three specific valves could not be used for each specimen, so all intact valves were included.

Growth Ring Counts

Valves were cross-sectioned using a Dremel® rotary tool with a diamond-coated cutting blade in order to observe growth rings. For each *C. stelleri* specimen, all valves were cut into quarter sections, on the long and short axes of the valve. Barring breakage, all sections of all valves were examined to assess growth rings (mean = 6 valves per specimen). Several of the dead, washed up specimens had broken valves that were unusable or which could only be measured in one direction. *Katharina tunicata* valves (valves 3, 4, 5) were also cut into quarter sections along the long and short axes. Valves of both species were then polished with increasingly fine silicone carbide grinding paper, with a final grit of 1,200.

Clear, dark growth rings were visible on *K. tunicata* valves with the naked eye after cross-sectioning and polishing (Fig. 5) and were counted under a dissecting microscope. Major growth rings in *C. stelleri* were not visible under a dissecting microscope so were examined via acetate peels following the protocol of Black et al. (2009). Acetate peels were taped to microscope slides and examined for growth rings on a compound light microscope. The distances between valve rings were measured using an eyepiece micrometer, and photos were taken of acetate peels using an Optixcam Summit 5.0 series® digital microscope camera. Photographs of valves were analyzed for the density of valve lines using the plot profile function in ImageJ in order to compare the growth of *C. stelleri* individuals from California, Oregon, and Washington. This was done by making transects down the middle of each valve and

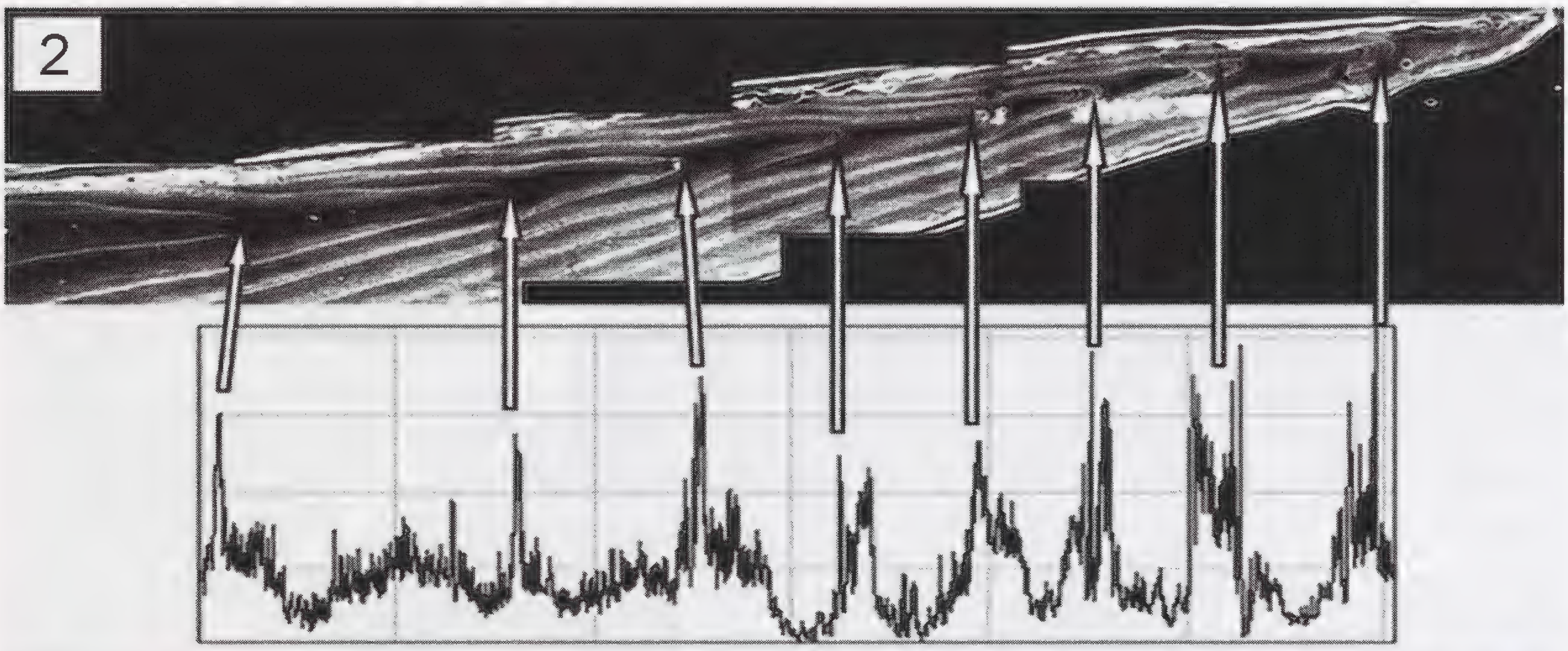

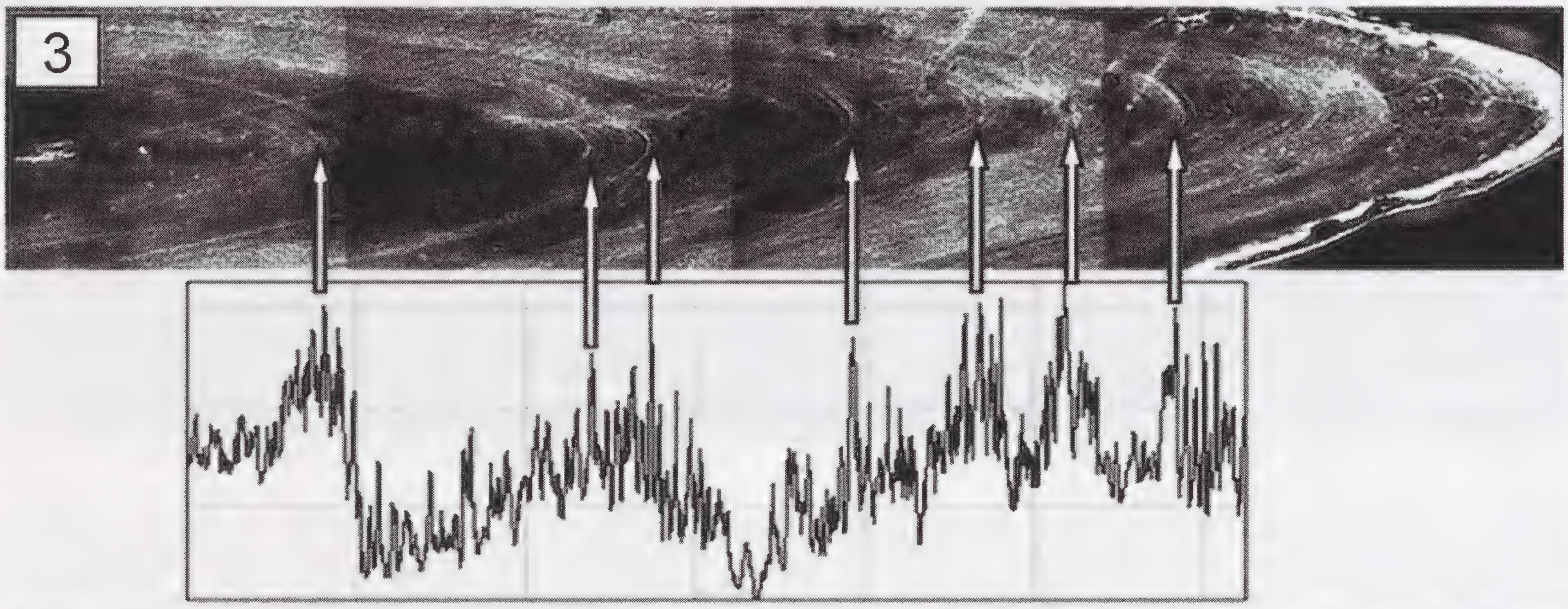

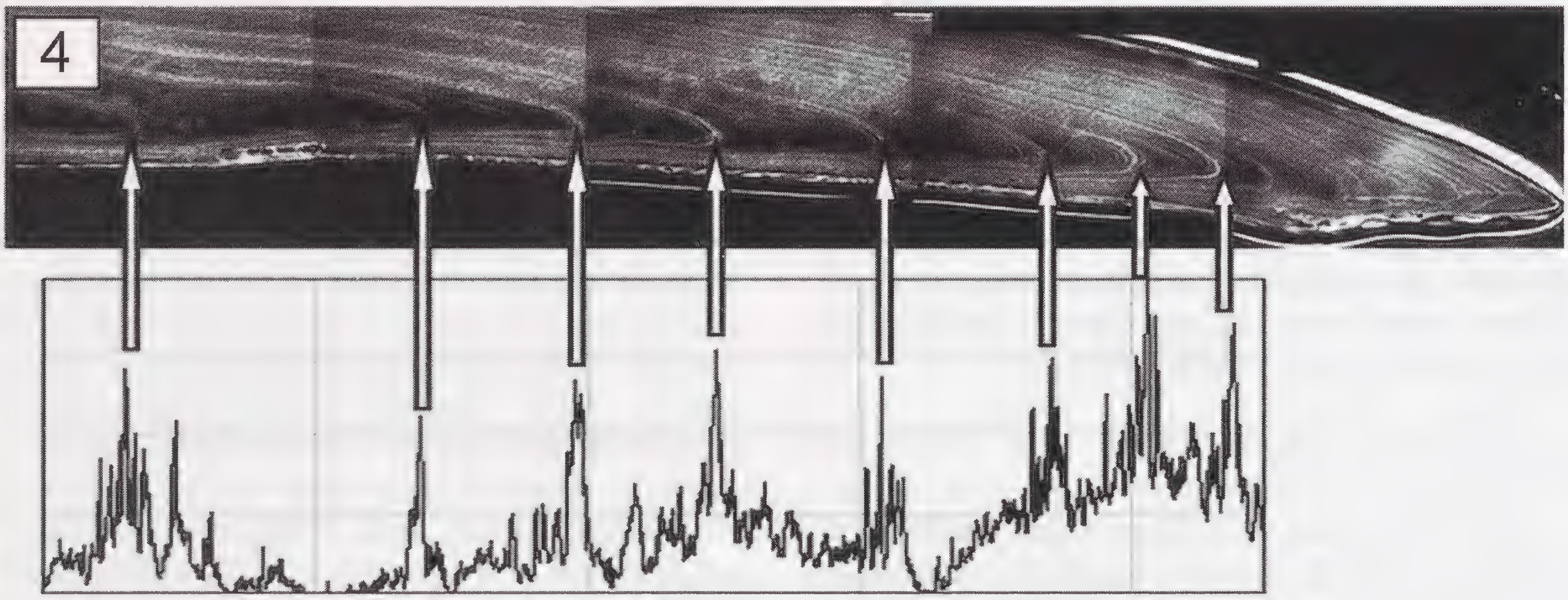

FIGS. 2–4. Photographs of acetate peels of sectioned *C. stelleri* valves from Washington, California, and Oregon. Graph shows associated plots of gray values from ImageJ, with peaks in gray value associated with each growth line because of the brightness of the line compared to the dark region of growth in between lines. Valves and graphs were chosen as representative examples of the differences in banding in the valves of Washington, Oregon and California specimens. FIG. 2: Acetate peel of valve cross-section from Washington. Growth lines are clearly defined, with very few smaller growth rings between major rings; FIG. 3: Acetate peel of valve cross-section from California. Growth lines are more obscure, with many pronounced smaller lines in between each growth band; FIG. 4: Acetate peel of valve cross section from Oregon. Growth lines are more clearly defined than California, but less clear than in individuals from Washington.

TABLE 1. All equations shown are the curves that were fit to size and age data for *Cryptochiton stelleri* and *Katharina tunicata*. Functions are shown that describe both the overall tissue growth and the shell (valve) growth of each species.

Species	y	x	Function	Equation	R^2
Katharina tunicata	Body Length (mm)		Von Bertalanffy	$y = 114 * (1 - e^{-0.217x})$	0.84
	Volume (mL)		Linear	$y = 7.83x - 10.6$	0.84
Cryptochiton stelleri	Circumference (cm)		Von Bertalanffy	$y = 39.4 * (1 - e^{-0.702x})$	0.97
	Volume (mL)	Age	Linear	$y = 32.1x - 79.4$	0.91
Katharina tunicata valves	Valve 4 Width (mm)		Von Bertalanffy	$y = 33.4 * (1 - e^{-0.172x})$	0.93
	Valve 4 Weight (g)		Power (2 param.)	$y = 0.167 * x^{1.20}$	0.83
Cryptochiton stelleri valves	Valve 8 Width (mm)		Von Bertalanffy	$y = 31.9 * (1 - e^{-0.0681x})$	0.72
	Valve 8 Weight (g)		Power (2 param.)	$y = 0.154 * x^{1.32}$	0.80

analyzing the gray values along this transect. The plot profile function plots gray values on a scale from zero (black) to 255 (white), with peaks in gray value indicative of a major growth ring (Figs. 2–4).

Growth lines faded out towards the center of the valves on older *C. stelleri* specimens, so an additive process was used to estimate the number of rings for these individuals. Since smaller specimens had all of their growth rings visible all the way to the center, the distance between each ring and the next was measured and a dataset was compiled that included the number of rings present at each distance from the center of the valve. These data were used (Figs. 6–8) to estimate the number of inner growth rings for those older individuals with growth rings that faded out towards the center of the valve. Growth increments were verified for *C. stelleri* using the list year technique described by Black et al. (2008), with conspicuously wide or narrow increments recorded and matched up between individuals of the same population.

Some *K. tunicata* individuals sampled were young enough (two growth rings) that there was not a large gap in the early part of the size-at-age curve for this species. However, no *C. stelleri* collected from any sites had fewer than four growth rings, leaving a gap in the early part of the size-at-age curve. Additional growth rate data for juvenile and young *C. stelleri* were used from Lord (2011b), who reported laboratory growth rates for juveniles of this species.

Size-at-Age Curves

Juvenile measurements of *C. stelleri* size at known age (Lord, 2011b) were combined with ring count information to create size-at-age curves showing the changes in several different morphological characteristics with age. Growth rings in *K. tunicata* appeared as conspicuous opaque bands, making growth ring counting much simpler, since acetate peels were not needed to discern the growth lines.

Growth data were plotted and fitted with appropriate curves in Sigmaplot® for both *C. stelleri* and *K. tunicata* (derived equations shown in Table 1). In order to create a complete size-at-age curve, data for *C. stelleri* specimens from Oregon sites were combined because they showed similar patterns. Separate size-at-age curves were created for *K. tunicata* from Oregon and *C. stelleri* from Washington, Oregon, and California.

RESULTS

No differences were found in valve growth rates of *C. stelleri* between Washington, Oregon, and California, although there were differences in the shell deposition patterns at these different locations. Growth ring counts estimated the lifespan of *Katharina tunicata* as at least 17 years, and *Cryptochiton stelleri* as at least 40 years. Both *K. tunicata* and *C. stelleri* displayed continuous growth in terms of age, volume, weight, and valve weight. Growth for both species in terms of body length and shell width slowed with age and approached an asymptote.

Growth Ring Counts

Acetate peels of *C. stelleri* valves showed clear major growth lines as bright (opaque) rings separated by dark (transparent) incre-

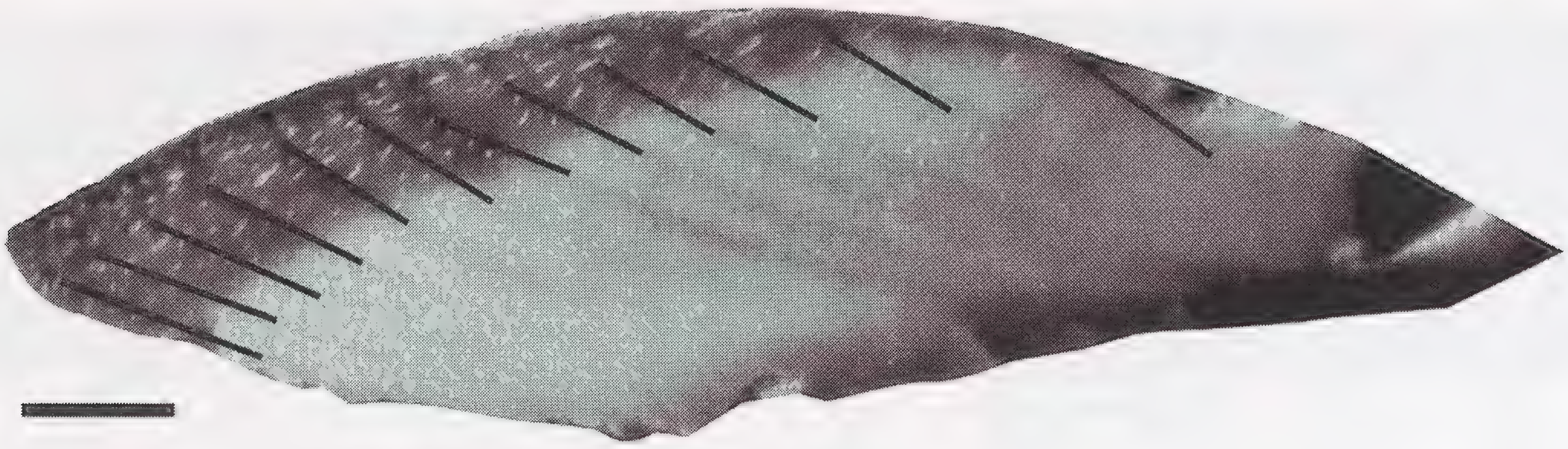

FIG. 5. Photograph of *K. tunicata* valve under a dissecting microscope (scale = 1 mm). Valve was cross-sectioned vertically (shown in Fig. 1) and then examined for major growth lines, which are each highlighted by overlaid black lines in the image.

ments of faster growth (Figs. 2–4). Spikes or peaks in the gray value in ImageJ coincided with major growth lines (Figs. 2–4) and helped to discern major growth rings. For *K. tunicata,* only major rings were visible under the dissecting microscope, so discerning between major and minor rings was not an issue. The additive method for counting rings (previously described) was fairly precise, as the curves estimating the numbers of growth rings to the center had a 95% confidence interval of approximately ± 2 rings (Figs. 6–8). Individual *C. stelleri* matched an average of 82% of the markers (conspicuously wide or narrow growth bands) selected for comparison by the list year technique. This ensured that the increments were aligned and made it more likely that age predictions were accurate across all specimens.

Cryptochiton stelleri valves from Fort Ebey, Washington (Fig. 2) showed very distinct growth rings, with very few smaller growth lines between the major annual bands. The major growth rings on the valves from Asilomar, California (Fig. 3), were much less pronounced and were obscured by a large number smaller growth rings clumped around each major ring. This distinction between Washington and California is clear on both the acetate peels and the gray value graphs. Valves from Oregon (Fig. 4) showed distinct growth lines similar to those from Washington, but slightly less defined.

There were no significant differences in spacing between major growth rings in valves from the three different states ($p > 0.3$). However, there were differences (one way ANOVA, df = 110, F = 15.39, $p < 0.0001$) in the dispersion of smaller growth rings around each major growth band. Each growth band is made up of a series of small (subannual) rings that form “bands” when they are spaced very closely together, indicative of periods of slow growth (winter). Both Washington (Tukey’s HSD, $p < 0.01$) and Oregon (Tukey’s HSD, $p < 0.01$) had growth lines that were significantly more tightly clustered (width of peak in gray value) than in the California valves. These tightly clustered minor growth lines made major growth bands in Washington and Oregon valves very distinct. Valves from Oregon *C. stelleri* specimens were not significantly different from Washington valves with regard to the clustering (of small growth marks around major growth rings (t-test, $p > 0.2$).

Size-at-Age Curves

Counts of the major growth rings were used to create size-at-age curves for *C. stelleri* and *K. tunicata*. Using ages inferred from the growth rings, body circumference of *C. stelleri* and length of *K. tunicata* were plotted against age, with juvenile *C. stelleri* data included from Lord (2011b) (Figs. 9, 10). The circumference-age or length-age data for both species were fit well ($r^2 = 0.84$ for *K. tunicata*, 0.97 for *C. stelleri*) (Table 1) by the von Bertalanffy growth function (von Bertalanffy, 1938), which is commonly used to describe growth of intertidal organisms (e.g., Ebert & Russell, 1992; Steffani & Branch, 2003) and is shown here: $L_i = L_\infty (1 - e^{-kt})$. L_i is body length, L_∞ is maximum or asymptotic body length, k is the instantaneous growth rate, and t is age.

Body volume was also plotted against estimated age, producing a different shaped curve for both species than the curves based on length and circumference (Figs. 9, 10). In both species, size, as measured by volume, increased continuously with age and was fit with a linear function ($r^2 = 0.84$ for *K. tunicata*, 0.91 for *C. stelleri*) (Table 1). Valve growth showed similar patterns (Figs. 11, 12), as valve weight growth rates actually increased with age for both spe-

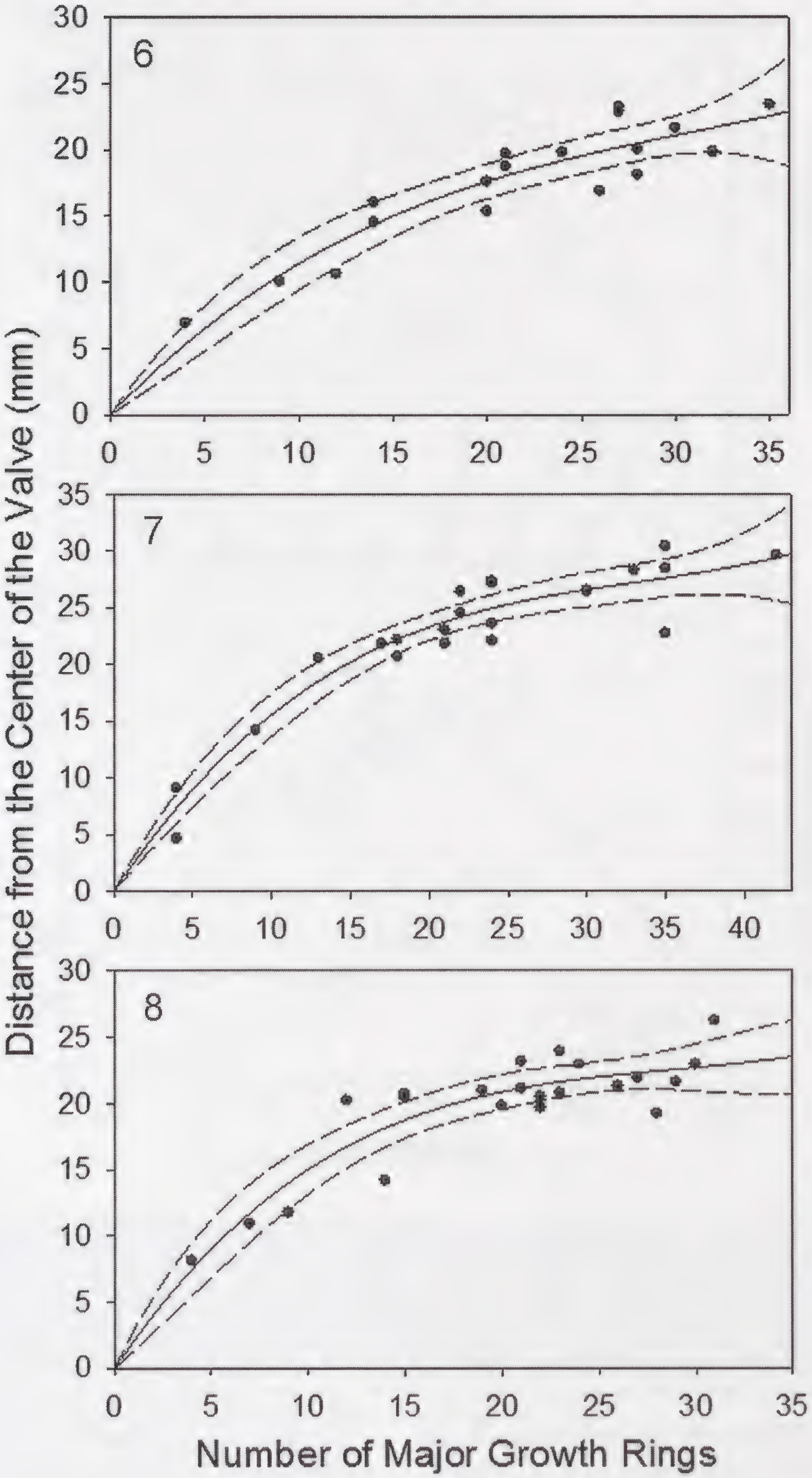

FIGS. 6–8. Curves used to help estimate the number of *C. stelleri* growth rings when valves had growth rings that faded towards the center. These curves were used to predict the number of rings that would be in that distance to the center of the valve. Data were fit with three parameter polynomial functions to describe patterns. 95% confidence intervals are shown on each graph. FIG. 6: Valve 1; FIG. 7: Valve 7; FIG. 8: Valve 8.

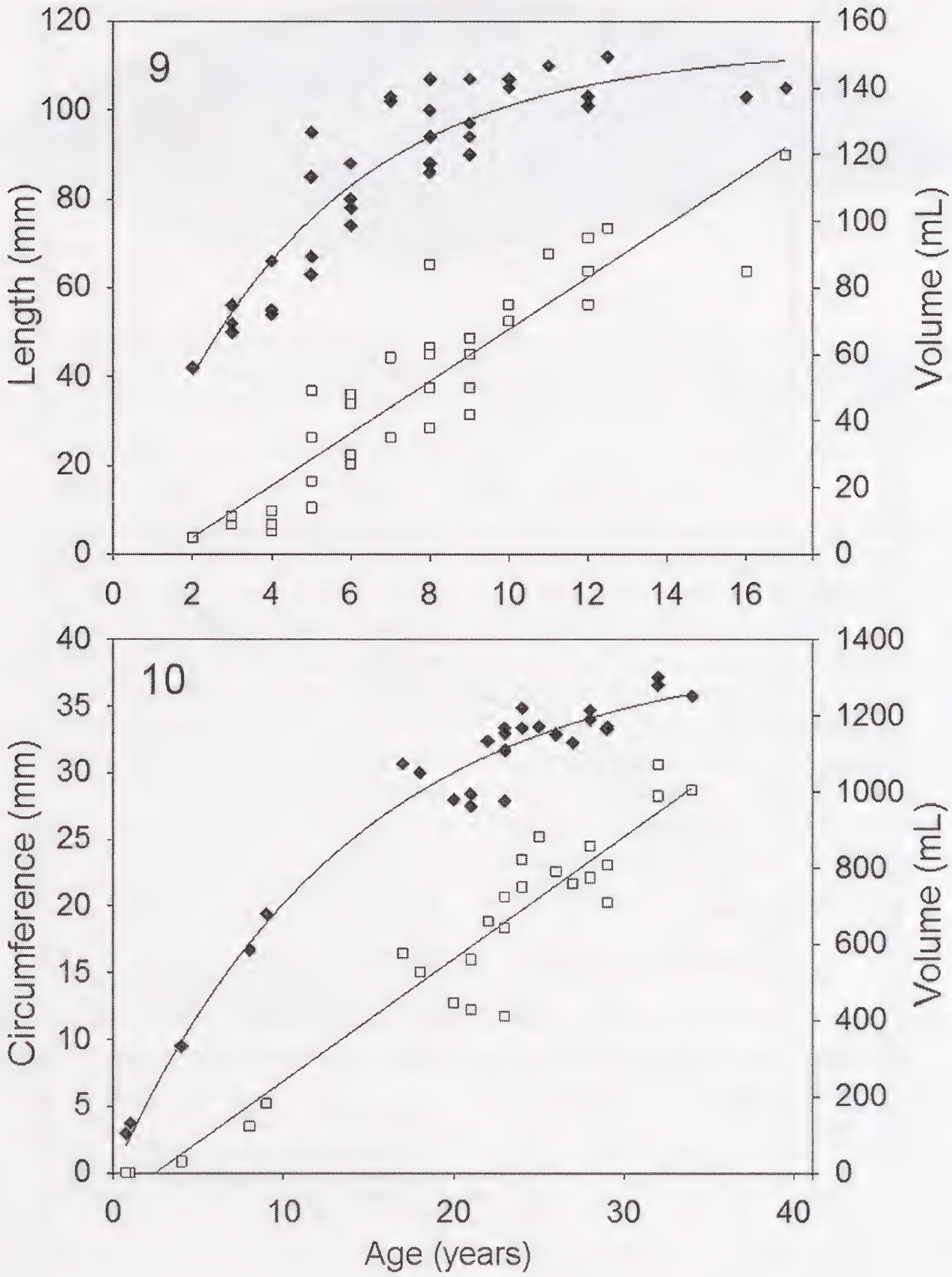

FIGS. 9, 10. Size-at-age curves based on volume and length (*K. tunicata*) or circumference (*C. stelleri*). Body length and body volume are both plotted against presumptive annual growth rings. Data are fit with growth functions described in Table 1. FIG. 9: Size-at-age curves for *K. tunicata* (n = 35); FIG. 10: Size-at-age curves for *C. stelleri* (n = 27). Circumference is used as a linear measure of size instead of length because of the flexibility of the organism.

cies and were fit with two-parameter power functions ($r^2 = 0.83$ for *K. tunicata*, 0.80 for *C. stelleri*) (Table 1). Valve width growth slowed with age in both species and was fit with the von Bertalanffy growth function ($r^2 = 0.93$ for *K. tunicata*, 0.72 for *C. stelleri*) (Table 1). These data included the datasets from Washington and California *C. stelleri* specimens, since they showed similar growth patterns to those from Oregon.

The size-at-age curves created for *K. tunicata* estimate that the oldest specimen sampled in this study was 17 years old. For *C. stelleri*, the oldest specimen sampled was approximately 42 years old. Both species have maximum recorded sizes larger than those used in the this study, so these lifespan estimates are likely underestimates of the longest possible lifespan for these species.

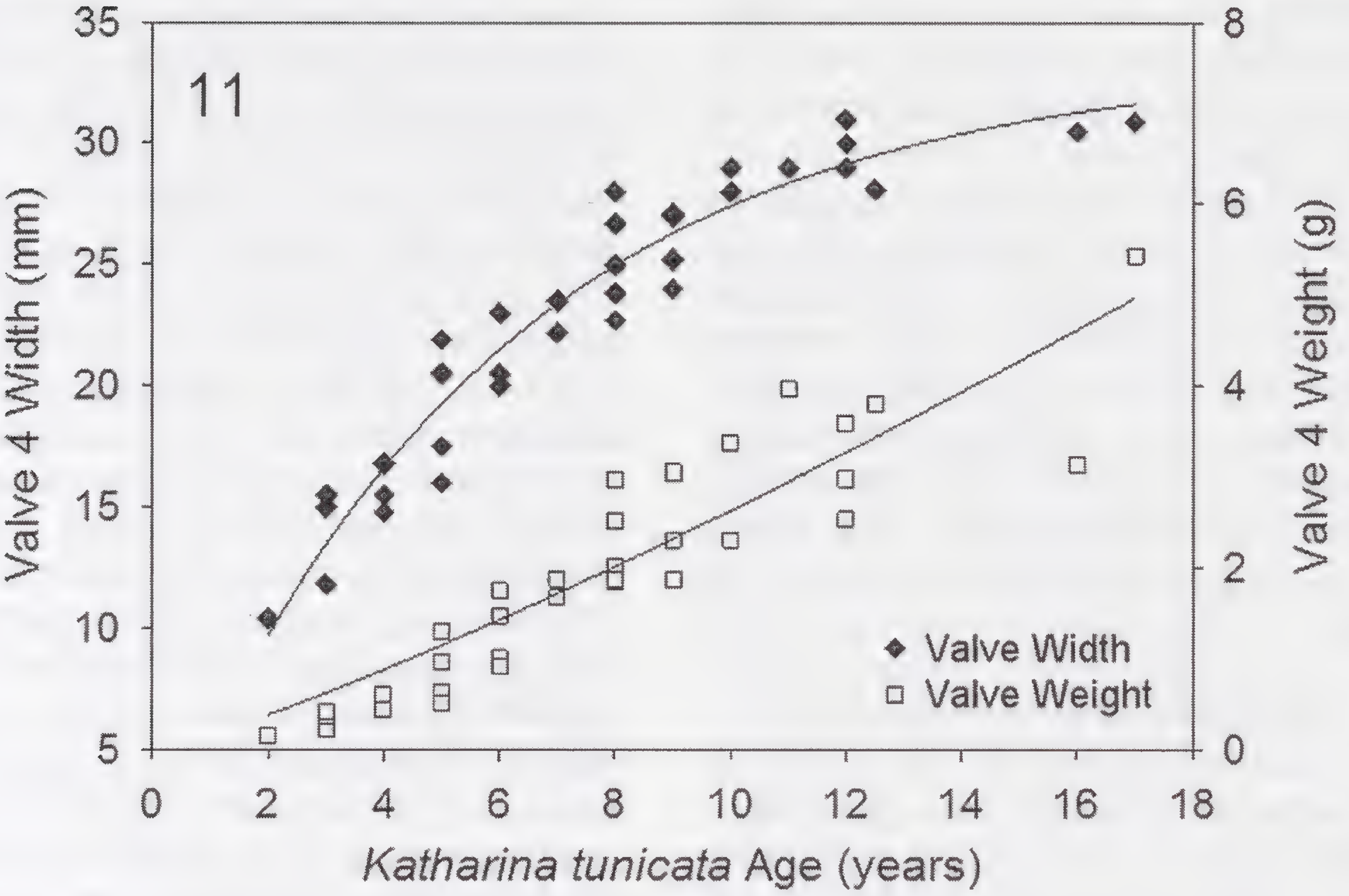

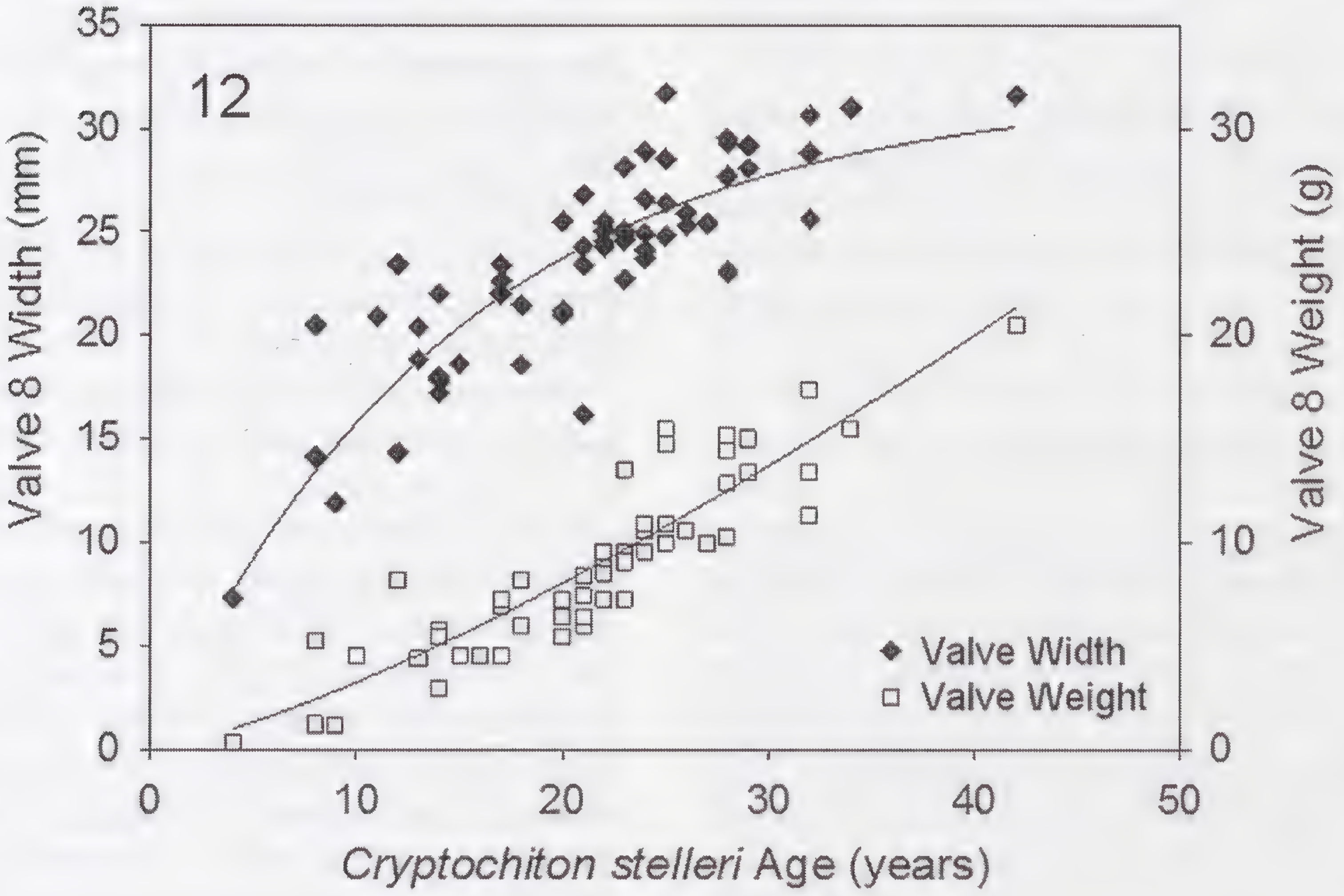

FIGS. 11, 12. Size-at-age curve for age and valve width and valve weight data for combined Washington, Oregon and California specimens of *C. stelleri* and Oregon specimens of *K. tunicata*. For both species, the valve width growth rate slows with age, while the valve weight growth rate increases with age. Data were fit with functions given in Table 1. FIG. 11: Size-at-age curve for *C. stelleri* valve 8 width and valve 8 weight plotted against presumptive annual growth rings; FIG. 12: Size-at-age curve for *K. tunicata* valve 4 width and valve 4 weight plotted against presumptive annual growth rings.

DISCUSSION

Several methods have been used to measure chiton growth, including measurements of valve width (Soliman et al., 1996), body length (Glynn, 1970), body weight (Palmer & Frank, 1974), external shell markings (Crozier, 1918; MacGinitie & MacGinitie, 1968) and internal growth rings (Jones & Crisp, 1985). Previous studies on the life histories of *Cryptochiton stelleri* and *Katharina tunicata* have been inconclusive regarding the growth rates and lifespans of these large chitons (Heath, 1905; MacGinitie & MacGinitie, 1968; Palmer

& Frank, 1974). The analysis of internal shell growth lines in this study resulted in the first accurate description of growth patterns for *C. stelleri* and *K. tunicata*.

Sclerochronology is becoming commonplace in growth studies of hard-shelled mollusks, especially bivalves (e.g., Schone, 2003; Black et al., 2008). Some of the difficulties involved in using this method of age determination are in confirming the assumption that growth rings are deposited regularly and determining the time interval between growth lines. In addition, it can be difficult to discern individual growth lines, making this process potentially subjective (Campana, 2001). Distinguishing between major growth lines was not difficult in the present study because of the clarity of these lines, with large transparent gaps in-between opaque rings (Figs. 2–4). Major growth lines were clearly visible in polished valve cross-sections for *K. tunicata* (Fig. 5) and in acetate peels for *C. stelleri*.

Growth increments in the valves of *K. tunicata* and *C. stelleri* were laid down at regular intervals, as evidenced by the clear distinction between periods of slow and fast growth. The use of several valves from the same individual to confirm growth ring counts also indicated regular increments of shell deposition. This was further confirmed by the list-year technique (Black et al., 2008) with *C. stelleri*, which matched conspicuously wide and narrow growth increments between individuals and between valves of the same individual. The matching of 82% of these markers across all specimens not only verified age estimates but also showed population-wide patterns of shell deposition that would likely not occur if growth rings were deposited inconsistently.

In order for growth ring counts to be reliably converted to age estimates and used to create growth curves, it was necessary to establish annual shell deposition. Annual growth rings are commonly formed during winter, when a slowdown in growth can result from gonad production, colder temperatures, increased storms, and lower food availability (Crozier, 1918; Baxter & Jones, 1978; Brousseau, 1979; MacDonald & Thomas, 1980; Picken, 1980; Thompson et al., 1980). The production of annual growth rings is especially common among organisms with annual food supplies, such as phytoplankton or macroalgae. *Cryptochiton stelleri* and *Katharina tunicata* spawn once per year in the spring (Giese et al., 1959; Tucker & Giese, 1962; Himmelman, 1978; Yates, 1989) and feed predominantly on seasonally abundant macroalgae (Dethier & Duggins, 1984; Yates, 1989), so it is likely that both species have a lower food intake in the winter and allocate most energy to gonad production. Therefore, shell growth should be minimal during this time, resulting in tightly clustered minor growth lines that appear as well-defined major growth bands deposited annually in the winter.

The finding that *Cryptochiton stelleri* valves between the sites in Washington, Oregon, and California on the west coast of the United States showed no significant differences in growth ring spacing indicates similar growth rates between these three locations. This suggests that shell deposition (and volumetric growth, by proxy) does not vary with latitude through this subset of the range of *C. stelleri*. However, the inclusion of only three locations precludes the ability to draw wide-scale latitudinal conclusions based on the present study. In addition, the 1,600 kilometer distance between the southern (California) and northern (Washington) sites are still only a small segment of the range of this species. Since the range of *C. stelleri* extends as far north as the Aleutian Islands and Kamchatka, it may display altered growth patterns in the different climactic regimes that it inhabits.

Some variation in *C. stelleri* shell deposition with latitude was evident in the difference found in the dispersion of smaller (minor) growth rings around major annual rings in the California valves compared to those from Washington and Oregon. Since major shell growth bands are collections of tightly spaced smaller minor growth lines, more widely dispersed minor lines, such as those found on California valves, indicate less seasonal differences in growth. This is supported by seasonal patterns in macroalgal abundance, since such macroalgae as *Mazzaella splendens* (a preferred food of *C. stelleri*) are seasonal in Washington and Oregon but present year-round in Monterey, California (Dyck & DeWreede, 2006). While *C. stelleri* can go months without feeding in Oregon where macroalgae is largely seasonal (Yates, 1989), it is likely that this species feeds year-round in California, resulting in the less-defined major growth bands. Since the acetate peel technique and multiple sites were not used for *K. tunicata*, minor growth lines were not analyzed, but similar latitudinal patterns would be expected based on range and feeding habits.

The presumptive conclusion that growth rings in *C. stelleri* and *K. tunicata* are annual allowed for the creation of size-at-age curves and longevity estimates for these species. In terms of length and shell width, both species displayed asymptotic growth patterns, which are commonly described by the von Bertalanffy growth function (Figs. 9–12). The length of *K. tunicata* (Fig. 9) leveled off more with age than did *C. stelleri* circumference (Fig. 10), but this may be a result of the size and age of specimens included in this study. The largest *K. tunicata* in this study was 11 cm long, compared to a maximum length of 12 cm for this species (Himmelman, 1978). In contrast, the longest *C. stelleri* included was approximately 25 cm, compared to a species maximum of 36 cm. Therefore, *C. stelleri* data may have shown the same pattern of minimal linear growth if larger individuals were included. In terms of volume and shell weight, growth was continuous or even increasing with age for both species (Figs. 9–12). It was clearly possible for both species of chiton to show increases in overall growth rate and shell deposition even as linear growth (shell width, body length) slowed down. These differing patterns are expected because volume generally varies as the cube of length, but it is interesting to note that both *C. stelleri* and *K. tunicata* do not slow down their volumetric growth rate even at advanced ages. This could be an adaptation to allow for increased feeding or reproductive output with age, but requires further study.

The longevity estimates for both *C. stelleri* and *K. tunicata* were much longer than previously reported by Heath (1905) or other studies in the case of *C. stelleri* (MacGinitie & MacGinitie, 1968; Palmer & Frank, 1974). The study by Heath (1905) was a largely anecdotal report that did not quantitatively assess growth rates of these species but instead made estimates based on sizes observed in the field. Growth rates and lifespans determined in this fashion are often underestimates, since linear growth slows with age (Figs. 9–12), making differences of even five years nearly imperceptible without detailed analysis. It is typical for estimates of lifespans based on sclerochronology to exceed previous estimates, especially for slow growing species such as the ocean quahog *Arctica islandica* (Strahl et al., 2007) and the Pacific geoduck *Panopea abrupta* (Black et al., 2008). This is due to the level of detail that can be observed in close examination of growth lines deposited in the shells. Studies such as the one by MacGinitie & MacGinitie (1968) that use external growth lines rely on obscure contours that can be altered by shell deterioration and can mask more detailed patterns. The difference between external growth lines and internal is illustrated by contrasting Figure 1 (external) with Figures 2–5 (internal), which show an immense level of detail, especially in the acetate peels of *C. stelleri* (Figs. 2–4). The use of internal growth lines for *Cryptochiton stelleri* and *Katharina tunicata* allowed for a detailed analysis of their growth patterns and thus served as a useful tool for age determination. Sclerochronology could be applied to further understanding annual and sub-annual patterns of shell deposition in *C. stelleri* and *K. tunicata* as well as other chiton species.

ACKNOWLEDGMENTS

This material is based upon work supported by the National Science Foundation under Grant No. 0638731, 2009–2010, PI's Alan Shanks and Jan Hodder. Collections were made with ODFW collecting permit #15387. I wish to thank Dr. Alan Shanks for supplying both advice and the dead *C. stelleri* specimens from California. Additional thanks to Dr. Cynthia Trowbridge for help with the manuscript and to Zair Burris for assistance with field collections.

LITERATURE CITED

ABELE, D., T. BREY & E. PHILLIP, 2009, Bivalve models of aging and the determination of molluscan lifespans. *Experimental Gerontology*, 44: 307–315.

BAXTER, J. M. & A. M. JONES, 1978, Growth and population structure of *Lepidochitona cinereus* (Mollusca: Polyplacophora) infected with *Minchinia chitonis* (Protozoa: Sporozoa) at Easthaven, Scotland. *Marine Biology*, 46: 305–313.

BLACK, B. A., C. A. COPENHEAVER, D. C. FRANK, M. J. STUCKEY & R. E. KORMANYOS, 2009, Multi-proxy reconstructions of northeastern Pacific sea surface temperature data from trees and Pacific geoduck. *Palaeogeography, Palaeoclimatology, and Palaeoecology*, 278: 40–47.

BLACK, B. A., D. C. GILLESPIE, S. E. MacLELLAN & C. M. HAND, 2008, Establishing highly accurate production-age data using the tree-ring technique of crossdating: a case study for Pacific geoduck (*Panopea abrupta*). *Canadian Journal of Fisheries and Aquatic Sciences*, 65: 2572–2578.

BROUSSEAU, D. J., 1979, Analysis of growth rate in *Mya arenaria* using the Von Bertalanffy equation. *Marine Biology*, 51: 221–227.

CAMPANA, S. E., 2001, Accuracy, precision and quality control in age determination, including a review of the use and abuse of age validation methods. *Journal of Fisheries Biology*, 59: 197–242.

CROZIER, W. J., 1918, Growth and duration of life of *Chiton tuberculatus*. *Proceedings of the National Academy of Science USA*, 4: 322–325.

DeBUSK, B. C., S. S. CHIMOTE, J. M. RIMOLDI & D. SCHENK, 2000, Effect of the dietary brominated phenol, lanasol, on chemical biotransformation enzymes in the gumboot chiton *Cryptochiton stelleri* (Middendorff, 1846). *Comparative Biochemistry and Physiology Part C*, 127: 133–142.

DETHIER, M. N. & D. O. DUGGINS, 1984, An "indirect commensalism" between marine herbivores and the importance of competitive hierarchies. *American Naturalist*, 124(2): 205–219.

DYCK, L. J. & R. E. DEWREEDE, 2006, Reproduction and survival in *Mazzaella splendens* (Gigartinales, Rhodophyta). *Phycologia*, 45(3): 302–310.

EBERT, T. A. & M. P. RUSSELL, 1992, Growth and mortality estimates for red sea urchin *Strongylocentrotus franciscanus* from San Nicolas Island, California. *Marine Ecology Progress Series*, 81: 31–41.

GANG, H., B. FENG, L. HUOSHENG & Z. JUNFENG, 2008, Age and growth characteristics of crimson sea bream *Paragyrops edita* Tanaka in Beibu Gulf. *Journal of the Ocean University of China*, 7: 457–465.

GIESE, A. C., J. S. TUCKER & R. A. BOOLOOTIAN, 1959, Annual reproductive cycles of the chitons *Katharina tunicata* and *Mopalia hindsii*. *Biological Bulletin*, 117: 81–88.

GLYNN, P. W., 1970, On the ecology of the Caribbean chitons *Acanthopleura granulata* Gmelin and *Chiton tuberculatus* Linne: density, mortality, feeding, reproduction, and growth. *Smithsonian Contributions to Zoology*, 66: 23 pp.

HEATH, H., 1905, The breeding habits of chitons of the Californian coast. *Zoological Anzeiger*, 29: 390–393.

HIMMELMAN, J. H., 1978, The reproductive cycle of *Katharina tunicata* Wood and its controlling factors. *Journal of Experimental Marine Biology and Ecology*, 31(1): 27–41.

JONES, P. & M. CRISP, 1985, Microgrowth bands in chitons: evidence of tidal periodicity. *Journal of Molluscan Studies*, 51: 133–137.

LORD, J. P., 2011a, Fine-scale intertidal distribution and recruitment patterns of the gumboot chiton *Cryptochiton stelleri* (Polyplacophora: Mopaliidae). *Malacologia*, 54: 147–157.

LORD, J. P., 2011b, Larval development, metamorphosis and early growth of the gumboot chiton *Cryptochiton stelleri* (Middendorff, 1847) (Polyplacophora: Mopaliidae) on the Oregon coast. *Journal of Molluscan Studies*, 77: 182–188.

MacDONALD, B. A. & M. L. H. THOMAS, 1980, Age determination of the soft-shell clam *Mya arenaria* using shell internal growth lines. *Marine Biology*, 58: 105–109.

MacGINITIE, G. E. & N. MacGINITIE, 1968, Notes on *Cryptochiton stelleri* (Middendorff, 1846). *The Veliger*, 11(1): 59–61.

O'FARRELL, M. R. & L. W. BOTSFORD, 2005, Estimation of change in lifetime egg production from length-frequency data. *Canadian Journal of Fisheries and Aquatic Sciences*, 62: 1626–1639.

PALMER, J. B. & P. W. FRANK, 1974, Estimates of growth in *Cryptochiton stelleri* (Middendorff, 1846) in Oregon. *The Veliger*, 16(3): 301–304.

PICKEN, G. B., 1980, The distribution, growth, and reproduction of the Antarctic limpet *Nacella* (*Patinigera*) *concinna* (Strebel, 1908). *Journal of Experimental Marine Biology and Ecology*, 42: 71–85.

SCHONE, B. R., 2003, A 'clam-ring' master-chronology constructed from a short-lived bivalve mollusc from the northern Gulf of California, USA. *Holocene*, 13: 39.

SOLIMAN, F. E., M. A. HUSSEIN, A. ALMARAGHY & T. HABIB, 1996, Population structure and growth curve of Acanthopleura gemmata (Mollusca: polyplacophora) in the northwestern Red Sea. *Qatar University Science Journal*, 16(2): 307–314.

STEFFANI, C. N. & G. M. BRANCH, 2003, Growth rate, condition, and shell shape of *Mytilus galloprovincialis*: responses to wave exposure. *Marine Ecology Progress Series*, 246: 197–209.

STRAHL, J., E. PHILIPP, T. BREY, K. BROEG & D. ABELE, 2007, Physiological aging in the Icelandic population of the ocean quahog *Arctica islandica*. *Aquatic Biology*, 1: 77–83.

THOMPSON, I., D. S. JONES & D. DREIBELBIS, 1980, Annual internal growth banding and life history of the ocean quahog *Arctica islandica* (Mollusca: Bivalvia). *Marine Biology*, 57: 25–34.

TUCKER, J. S. & A. C. GIESE, 1962, Reproductive cycle of *Cryptochiton stelleri* (Middendorff). *Journal of Experimental Zoology*, 150(1): 33–43.

VON BERTALANFFY, L., 1938, A quantitative theory of organic growth (inquiries on growth laws II). *Human Biology*, 10: 181–213.

YATES, K. R., 1989, *Notes on the feeding ecology of the gumboot chiton*, *Cryptochiton stelleri* (Middendorff). PhD Thesis, Zoology, Oregon State University, [xiii] + 190 pp.

Revised ms. accepted 5 October 2011